Experimental investigation of the magnetochiral index in liquids

Thierry Ruchon, Marc Vallet,* Dominique Chauvat, and Albert Le Floch
Laboratoire d'Électronique Quantique-Physique des Lasers, Unité Mixte de Recherche du Centre National de la Recherche Scientifique 6627, Université de Rennes I, Campus de Beaulieu, F-35042 Rennes Cedex, France

Jean-Yves Thépot
Laboratoire Organométalliques et Catalyse, Unité Mixte de Recherche du Centre National de la Recherche Scientifique 6509, Université de Rennes I, Campus de Beaulieu, F-35042 Rennes Cedex, France
(Received 21 July 2005; published 25 October 2005)

We showed through experiments that the magnetochiral index is polarization invariant and reported its wavelength dependence. These properties were investigated with limonene and using a specially-designed Ar^+-ring active interferometer. A Fresnel drag-type optical bias inside the discharge tube, combined with two calibrations and the circumvention of systematic errors, allowed us to reach a detection level in the range of 10^{-12} when measuring the change in the magnetochiral index of intracavity liquid samples. Our results are in agreement with the different predictions made for magnetochiral refraction.

DOI: 10.1103/PhysRevA.72.043405 PACS number(s): 33.55.Fi, 33.15.Bh, 42.81.Pa

I. INTRODUCTION

Recently, magnetochirality has received much attention, both theoretically [1–4] and experimentally [5–8]. This fundamental interaction appears as a shift both in the absorption coefficient and in the optical index of a chiral medium subjected to a static magnetic field parallel to the direction of the propagation of light [9]. Magnetochirality has been suggested as one of the possible reasons for the origin of homochirality of life [10]. Indeed, it has been shown that it can give rise to small enantiomeric excesses through photolysis controlled by light and static magnetic fields [11]. Its sign is a function of the orientation of the light wave vector with respect to the magnetic field. In pure chiral liquids, such as limonene, for instance, the magnitude of the magnetochiral index, i.e., the shift in optical index, is predicted to be of the order of 10^{-11} for a magnetic field of 1 T [12].

The first experimental setup used to measure the magnetochiral index was based on a passive interferometer [6]. However, for the molecules tested, the experimental values of the magnetochiral index were much higher than the values computed by theoretical calculations [3]. Then, an active ring interferometer was designed to measure the magnetochiral index of molecules [7]. The values obtained with this apparatus appeared to be 20 times lower than those reported in Ref. [6]. Furthermore, several features of the magnetochiral index have not been studied so far. In particular, it is predicted that the magnetochiral interaction, and hence the magnetochiral index, is independent of the polarization characteristics of the light beam. Moreover, the wavelength dependence of the magnetochiral index has not been measured as yet. In this study, we investigated these properties to further validate the values obtained using the active interferometer.

The paper is structured as follows. In Sec. II we discuss the basic properties of the magnetochiral index. In Secs. III and IV we analyze in detail the experimental setup and discuss the improvements that have occurred since the publication of Ref. [7]. In Sec. V experimental results obtained for different polarizations and wavelengths are compared with the theoretical predictions. Section VI concludes the article.

II. PROPERTIES OF THE MAGNETOCHIRAL INDEX

Chiral media exhibit circular differential optical indices associated to natural optical activity. Media of any symmetry, but submitted to a longitudinal magnetic field **H**, also exhibit circular differential optical indices that lead to magnetic optical activity, i.e., Faraday effect. Moreover, if the medium submitted to **H** is chiral, a third effect also arises, which again consists in a variation of the optical index. This so-called magnetochiral interaction was implicitly mentioned in Ref. [13], and since then has been estimated for molecules in refraction [12], and in absorption and emission [14]. Recently, magnetochiral indices were computed at the Hartree-Fock wave-function level [3] or using a dipole-dipole interaction model [15]. The basic features of the interaction can be readily obtained from the analysis described in Ref. [12]. The relative dielectric tensor ε is expanded to the first order in the light wave vector **k** and in the external field **H**. Assuming $\mathbf{k}=k\mathbf{e}_z$ and $\mathbf{H}=H\mathbf{e}_z$, where $\mathbf{e}_z$ is a unit vector along the z axis of propagation, the relative dielectric constants ε_+ and ε_- for right and left circularly polarized light, respectively, are given by

$$\varepsilon_{\pm}(\omega,\mathbf{H},\mathbf{k}) = \varepsilon(\omega) \pm a_F(\omega)H \pm a_{OA}(\omega)k + a_{MC}(\omega)Hk. \tag{1}$$

In this expression, a_{OA} and a_F characterize the natural optical activity and the Faraday effect, respectively, and a_{MC} describes the magnetochiral index. It is a nonreciprocal scalar, in the sense that two counter-propagating waves experience opposite refractive indices. From symmetry considerations, a_{MC} is also shown to change sign with the handedness of the

*Electronic address: lpl@univ-rennes1.fr

chiral sample. There are also other properties that indicate the presence of the magnetochiral effect. From Eq. (1), the magnetochiral index does not depend on polarization. With regard to the wavelength dependence for large detuning from the absorption band and for an interaction length L, the difference in the refractive index Δn_{MC} for two counter-propagating waves can be evaluated from the angle of rotation due to the natural optical activity $\theta = k^2 L\, a_{AO}/2\sqrt{\varepsilon}$ [12]. Indeed, from Becquerel's formula for the Faraday effect extended to the treatment of the magnetochiral index, Δn_{MC} is given by

$$\Delta n_{MC} = n(\mathbf{H}\uparrow\uparrow\mathbf{k}) - n(\mathbf{H}\uparrow\downarrow\mathbf{k}) = \frac{a_{MC} H k}{\sqrt{\varepsilon}} \simeq -\frac{eH\lambda}{4\pi^2 mLc}\frac{\partial(\lambda^2\theta)}{\partial\lambda}, \tag{2}$$

where e and m are the charge and the mass of the electron, respectively, and λ is the wavelength. $\mathbf{H}\uparrow\uparrow\mathbf{k}$ and $\mathbf{H}\uparrow\downarrow\mathbf{k}$ denote parallel and antiparallel $\mathbf{H}$ and $\mathbf{k}$ vectors, respectively. We estimate Δn_{MC} from $\Delta n_{OA} = 2\theta/kL$, the difference of indices between left and right circularly polarized light due to natural optical activity. Far from resonance, at first order, the usual dependence of the rotation θ with λ is written as $\theta(\lambda) = \Theta_0/(\lambda^2 - \lambda_0^2)$, where Θ_0 is a constant [16]. For $H = 1$ T, $\lambda = 488$ nm and $\lambda_0 = 180$ nm, Eq. (2) leads to

$$\Delta n_{MC} = \frac{eH}{2\pi mc}\frac{\lambda}{\frac{\lambda^2}{\lambda_0^2} - 1}\Delta n_{OA} \simeq 7 \times 10^{-6}\Delta n_{OA}. \tag{3}$$

To investigate the properties of the magnetochiral index, we report experiments performed on limonene, mainly at $\lambda = 488$ nm. This pure chiral liquid is an optically stable compound that exhibits an optical density lower than 1.5 cm^{-1} at 488 nm. This low absorption is necessary to avoid cascade terms, thus probing true magnetochiral anisotropy in refraction [17]. The first absorption band is located at $\lambda_0 = 180$ nm. Pure liquid $S(-)$ and $R(+)$ limonene of 82% enantiomeric excess (e.e.) was used (Fluka Puriss Grade). The specific rotations at 488 nm were measured to be $-152°/\mathrm{dm}/(\mathrm{g\,mL}^{-1})$ and $152°/\mathrm{dm}/(\mathrm{g\,mL}^{-1})$, respectively. For the racemic mixture $R(+)$-$S(-)$, the residual specific rotation is measured to be lower than 0.5°. The expected magnetochiral index is thus in the range of 10^{-11} T^{-1} to 10^{-10} T^{-1} for optically active compounds.

III. RING LASER-BASED INTERFEROMETER

To measure the nonreciprocal difference of indices Δn_{MC}, we consider a ring laser with two counter-propagating waves oscillating in the clockwise (cw) and counter-clockwise (ccw) directions at frequencies ν_{cw} and ν_{ccw}. Any nonreciprocal contribution, $\Delta n_{NR} = n_{ccw} - n_{cw}$, to the index of refraction inside the laser cavity for the oppositely directed beams induces a shift $\Delta\nu$ in the frequency difference $\nu_{ccw} - \nu_{cw}$. We assume that (i) the two counter-propagating waves oscillate on the same longitudinal mode, (ii) the perimeter of the laser cavity, P, is much larger than the length L of the nonreciprocal medium, and (iii) the cold-cavity approximation is fulfilled, i.e., the correction to the beat note frequency due to pulling or pushing is negligible [18]. $\Delta\nu$ is then equal to

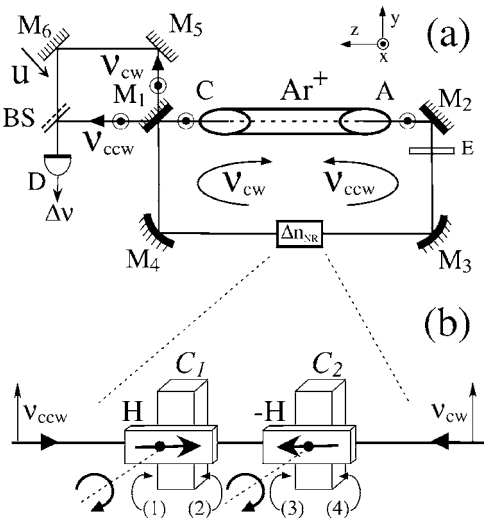

FIG. 1. (a) Schematic of the interferometer. Counter-propagating waves of frequencies ν_{ccw} and ν_{cw} oscillate inside a ring cavity (not to scale) made of four mirrors M_i ($i = 1,4$). They probe nonreciprocal optical index differences $\Delta n_{NR} = n_{ccw} - n_{cw}$. A beam splitter BS and two mirrors M_5 and M_6 combine the output beams onto a detector D to measure the beat note frequency $\Delta\nu$. M_6 can move at speed u to infer the sign of $\Delta\nu$. An Ar^+-ion discharge tube provides the gain. C, cathode; A, anode. (b) Detection of the magnetochiral birefringence: two cells C_1 and C_2, submitted to two rotating opposite magnetic fields H and $-H$ are inserted inside the cavity.

$$\Delta\nu = -\frac{cL}{\lambda P}\Delta n_{NR}. \tag{4}$$

In particular Δn_{MC} can be substituted for Δn_{NR} in expression (3) when one introduces, inside the cavity, a cell of length L filled with a medium exhibiting only the magnetochiral index.

Our experimental schematic is shown in Fig. 1(a). A ring cavity of perimeter $P = 3.66$ m is made of two plane mirrors M_1 and M_2 and two spherical mirrors M_3 and M_4 with a radius of curvature $R_c = 6$ m. The gain at $\lambda = 488$ nm is provided by an Ar^+ dc-discharge tube (Coherent Innova 70) on the $4p^2 D^0_{5/2} \rightarrow 4s^2 P_{3/2}$ transition of Ar^+ [19]. This transition has been selected because it presents a relatively high single-pass gain, measured to be 1.3 at a discharge current I of 20 A. It thus allows the insertion of intra-cavity samples. Moreover, Eq. (2) shows that Δn_{MC} depends on the dispersion of the optical activity, which is usually larger on the blue side of the spectrum. The Brewster windows closing the tube impose linear polarization of light inside the cavity along the x axis. An étalon E selects a single longitudinal mode for the two counter-propagating traveling waves. This has been checked using a Fabry-Perot interferometer.

To measure $\Delta\nu$, 2 mW output beams are recombined on a photodiode D using two mirrors M_5 and M_6 and a beamsplitter BS. The axial drift of the gas inside the tube induces a Fresnel drag-type optical bias $\Delta\nu_0$, which avoids the lock-in

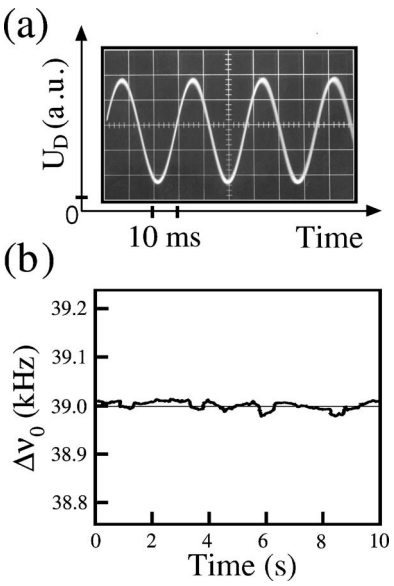

FIG. 2. (a) The beat note signal of the ring laser at 39 kHz. U_D, output voltage from D. (b) The baseline obtained by demodulating the beat note $\Delta\nu_0$. It presents root-mean-square variations $\Delta\nu_{rms}$ =8 Hz over 10 s.

region [18]. The resulting beat note signal is $\nu_{ccw}-\nu_{cw}$ $=\Delta\nu_0$ [Fig. 2(a)]. It is equal to 39 kHz and exhibits high stability. The beat note signal was obtained by isolating the experiment from acoustic vibrations, by circumventing thermal drifts and by shielding the discharge tube from external magnetic fields. Moreover, a resonance frequency of the cavity is locked to the optical frequency of a home-built single frequency He—Ne laser (not shown in Fig. 1). It is stabilized in frequency and intensity, and enables servocontrol of the ring cavity length over hours. Figure 2(b) shows the instantaneous beat note frequency of the signal on D versus time (measured with a HP 53310 A modulation domain analyzer). The root-mean-square frequency variations of $\Delta\nu$ are equal to $\Delta\nu_{rms}$=8 Hz over 10 s. Using expression (4) and a sample of length L=2 cm, the root-mean-square sensitivity $\langle\Delta n_{NR}\rangle_{rms}$ of the measurement of nonreciprocal indices equals 2×10^{-12}. Furthermore, mirror M_6 is mounted on a translation stage whose speed u can be monitored. When moving at u (Fig. 1), M_6 induces a Doppler frequency shift for ν_{cw}. From the signs of u and of the shift of $|\Delta\nu|$, one can infer the sign of $\Delta\nu$. The sign of Δn_{NR} is thus experimentally deduced from the beat note frequency $\Delta\nu$. For instance, below the lock-in region, $\Delta\nu_0$ is positive, which corresponds to a drift in the tube from the anode to the cathode.

Figure 3 shows the plot of the amplitude of the optical bias as a function of the discharge current I. We have superimposed the difference of pressure between the anode and the cathode versus I [20]. At first order, the drift velocity is proportional to this difference. It shows that the velocity of the active medium induces the observed optical bias. In addition, at our operating current of 20 A, the 39 kHz bias is located well outside the lock-in region of the ring laser. Finally, the fluctuations of the discharge current have been measured to be equal to I_{rms}=2 mA_{rms} when I=20 A. Figure 3 shows that the fluctuations of the bias due to the fluctuations of the current are of the order of 3 kHz A^{-1} for I =20 A, which results in $\Delta\nu_{rms}\simeq6$ Hz. The main source of fluctuations during the evolution of the beat note is thus the noise due to the discharge current.

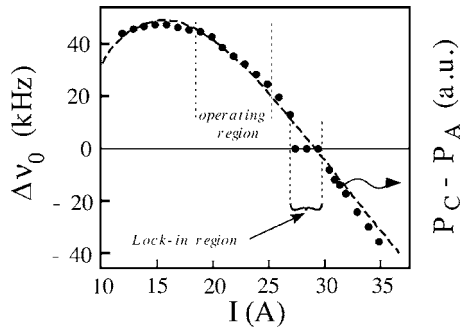

FIG. 3. Variations of the optical bias $\Delta\nu_0$ versus the discharge current I. Dots, measurements; dashed curve, pressure difference P_C-P_A between the anode and the cathode (from Ref. [20]), with arbitrary scales.

The experimental arrangement proposed to detect the magnetochiral birefringence of intracavity samples is depicted in Fig. 1(b). The intracavity cells C_1 and C_2 consist of two paired 1 cm-long fused silica cells. One cell is filled with one enantiomer of a chiral compound and the second with its opposite enantiomer. After traveling through both cells, the cw and ccw oscillating waves should not experience any rotation of the plane of polarization due to natural optical activity. Two identical magnets are set in front of the cells and induce opposite longitudinal magnetic fields **H** and **−H** in the optical path inside C_1 and C_2, respectively. The Faraday rotation should, therefore, also be cancelled after propagation through C_1 and C_2. Conversely, the contributions of the magnetochiral effect for C_1 and C_2 add up. We write a_{MC} (respectively, $-a_{MC}$) as the magnetochiral index associated to C_1 (respectively, C_2). Assuming that **H** and $\mathbf{k}_{cw}$ have the same direction, Eqs. (2) and (4) lead to

$$\Delta\nu=\Delta\nu_0-\frac{cL}{\lambda P}\Delta n_{MC}=\Delta\nu_0-\frac{2\pi cL}{\lambda^2 n_0 P}a_{MC}H, \qquad (5)$$

where n_0 is the isotropic and scalar part of the refractive index inside the cells. Equation (5) shows that the interferometer should enable one to deduce from $\Delta\nu$ both the amplitude and the sign of Δn_{MC}.

IV. CALIBRATION AND BASELINE

In this section, we carry out two calibrations with nonreciprocal effects and discuss, both theoretically and experimentally, polarization-induced systematic errors.

A. Sagnac and Fizeau effects

In order to calibrate the interferometer, independent nonreciprocal phase shifts are induced by rotating the whole cavity (Sagnac-type phase shift) and by moving an intracavity sample (Fizeau-type phase shift). During these experiments, an achiral species, water, was filled in both cells to avoid magnetochiral-related signals.

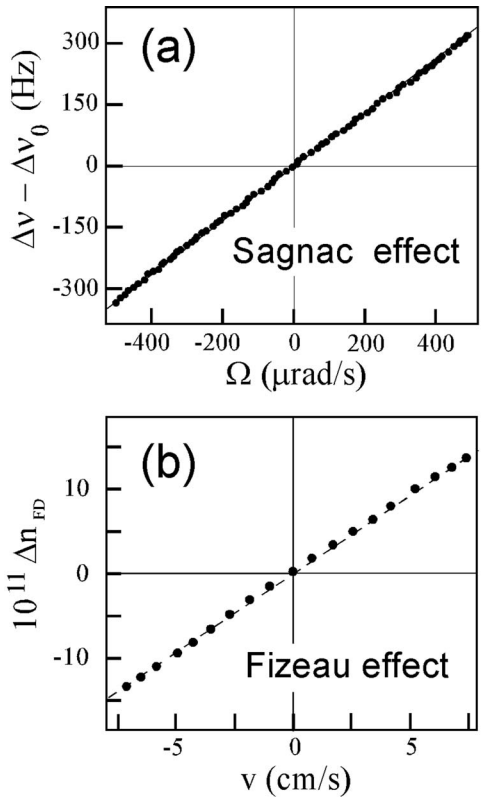

FIG. 4. (a) Observation of the Sagnac effect. Dots, experimental beat note frequency with respect to the angular frequency Ω of the ring interferometer; solid line, linear fit. (b) Observation of the Fresnel drag effect. Dots, experimental nonreciprocal index difference Δn_{FE} as a function of the speed v of the intracavity glass plate; dashed line, linear fit.

In the first experiment, the breadboard, on which the entire apparatus is mounted, is set in a rocking motion using a piezoelectric actuator. It leads to an alternating motion $\Theta(t)=\Theta_M \sin(\omega t)$, with $\omega/2\pi=1.1(\pm 0.1)$ Hz and $\Theta_M=15(\pm 3)$ μrad. The Sagnac-effect formula then gives [18]

$$\Delta\nu=\Delta\nu_0+\frac{4S}{\lambda P}\Omega, \tag{6}$$

where the area S enclosed by the light path is equal to 0.4 m^2 and the angular frequency Ω is equal to $\omega\Theta_M\cos(\omega t)$. It yields a theoretical scale factor $4S/\lambda P$ equal to 8.9×10^5 Hz/(rad s^{-1}). Figure 4(a) shows the evolution of the beat note as a function of Ω. The predicted linear relationship between the beat note frequency and the rotation rate is demonstrated. Moreover, a linear fit yields an experimental scale factor of $7.2(\pm 2)\times 10^5$ Hz/(rad s^{-1}), in agreement with Eq. (6).

In a second set of experiments, an intracavity glass plate, with thickness $L_p=4.9$ mm, is mounted on a motorized translation stage. It leads to a sinusoidal motion at a speed of $v(t)=v_M \sin(t)$. v_M is equal to 7.5 cm s^{-1} and $\omega/2\pi$ is equal to 1 Hz. To avoid the effects of multiple reflections inside the glass, the normal axis of the glass sample is tilted at an angle of 1° with respect to the cavity axis. The Fizeau effect generated by the motion of the glass induces a nonreciprocal phase shift that, again, manifests itself as a difference Δn_{FE} for the optical indices associated with the counterpropagating waves. It is shown that Δn_{FE} is, at first order, equal to $\Delta n_{FE}=-2(n^2-1)v/c$ [21]. The direction of v is given by the direction of propagation of the cw wave. The beat note frequency is then written as

$$\Delta\nu=\Delta\nu_0+2(n^2-1)\frac{L_p v}{\lambda P}. \tag{7}$$

Figure 4(b) shows the linear evolution of the experimental beat note frequency versus v. A linear fit gives a slope equal to $55(\pm 10)$ Hz/(cm s^{-1}), in agreement with the 64 Hz/(cm s^{-1}) expectation obtained from Eq. (7). These two calibrations prove (i) the sensitivity of our apparatus to nonreciprocal effects and (ii) the validity of expression (5) obtained using a cold-cavity model.

B. Baseline and systematic errors

The values of the magnetochiral index are deduced from Eq. (5). This expression has been derived from a scalar model of the ring laser. However, polarization effects, both circular and linear, may also induce beat note variations that could alter the experimental values and should, therefore be circumvented. They are investigated in this section.

First, the intracavity samples necessarily present natural and magnetic circular birefringence, whose corresponding index shifts are about three orders of magnitude higher than the magnetochiral index. These polarization effects are cancelled out after propagation through both cells. Indeed, the use of paired cells ensures that the associated optical paths are equal. Specific optical rotations of our samples are checked with a precision better than 1%. To balance the Faraday rotations, we use paired Nd-Fe-B permanent magnets. They are mounted on rotating posts to modulate (at 1 Hz) the component of **H** parallel to **k**. When an achiral sample, water or a racemic solution, is filled in both cells, the rotation of magnets should not change the beat note frequency. This baseline allows the adjustment of the position of the magnets in front of the cells so that the magnetic fields are opposite on the light path.

Second, linear birefringences can induce beat note variations. For instance, we noticed that some residual variations following the rotation of the magnets may still remain, depending on the position of the laser spot on the cells. This systematic effect is actually due to residual strain birefringence inside the cells windows. Using a vectorial description of the laser [22], based on the Jones formalism [23], Eq. (5) becomes, as presented in Appendix A,

$$\Delta\nu=\Delta\nu_0-\frac{cL}{\lambda P}\Delta n_{MC}+\Delta\nu_\varphi, \tag{8}$$

where the extra term $\Delta\nu_\varphi$ is given by

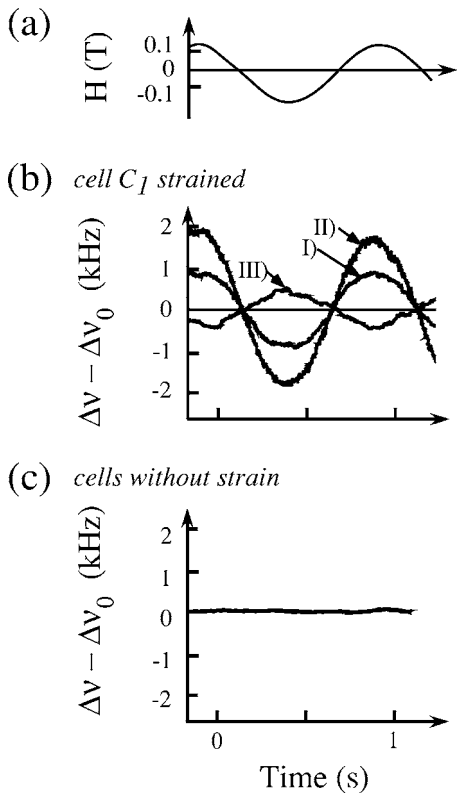

FIG. 5. (a) Longitudinal magnetic field H versus time when the magnets rotate. (b) Beat note frequency versus time when cell C_1 is strained. Curve I: C_1 and C_2 are filled with racemic limonene; Curve II, C_1 is filled with $R(+)$ limonene and C_2 with $S(-)$ limonene. Curve III, C_1 is filled with $S(-)$ limonene and C_2 with $R(+)$ limonene. (c) Baseline, beatnote frequency when both cells are filled with racemic limonene and strain is not applied.

$$\Delta\nu_\varphi \simeq \frac{c}{P}\frac{\varphi\theta_F}{\pi}\frac{\sin(2\psi-\chi)}{\cos\chi} - 2\frac{c}{P}\frac{\varphi\theta_F\theta_{OA}}{\pi}\cdot\frac{\cos(2\psi-\chi)}{\cos\chi}. \tag{9}$$

In this equation, θ_F (respectively, θ_{OA}) is the rotation of the plane of polarization experienced by the ccw wave through the sample inside C_1 due to the Faraday effect (respectively, the optical activity). φ is the effective retardance due to the residual linear birefringence inside the four windows of the cells. ψ and χ are angles depending on the orientation of the associated neutral axes. It shows that $\Delta\nu_\varphi$ is associated with a cross effect between linear and circular birefringence, i.e., it is proportional to the product $\varphi\theta_F$.

To experimentally validate expression (9), cell C_1 is artificially strained to increase φ. The induced retardance is independently measured to be $\varphi=20(\pm5)$ mrad. In a first set of experiments, both cells are filled with a racemic mixture of $R(+)$ and $S(-)$ limonene, i.e., θ_{OA} is set to zero in expression (9). Curve (I) of Fig. 5(b) is the corresponding baseline. It shows that $\Delta\nu_\varphi$ is linear with respect to the magnetic field, which is reported in Fig. 5(a). This is in agreement with expression (9). In a second set of experiments, $R(+)$ [respectively, $S(-)$] limonene is filled in cell C_1 (respectively, C_2). The beat note evolution obtained is curve (II) in Fig. 5(b). We find that the beat note amplitude increases because of the contribution of the second term in Eq. (9), which adds to the baseline. Finally, interchanging the samples in the cells, θ_{OA} becomes $-\theta_{OA}$ in Eq. (9). Now, the contribution of the second term has to be subtracted from the baseline, in agreement with the beat note evolution displayed by curve (III) in Fig. 5(b). The amplitude of the intracavity retardance is then deduced using Eq. (9). Measurements reported in Fig. 5(b) lead to $\Delta\nu_\varphi=1.2$ kHz. The 0.13 T magnetic field induces a rotation θ_F equal to 5.2 mrad for limonene; θ_{OA} is equal to 265 mrad. By assuming $\chi\ll1$ and $\chi\ll1$, and neglecting contributions of Δn_{MC} to the beat note frequency, Eq. (9) yields $\varphi=16$ mrad, as expected from our independent measurement.

Without artificial strain, the typical residual retardance of a 1 mm-thick cell window is of the order of 5 mrad. Such retardance would induce a variation $\Delta\nu_\varphi$ of the beat note in the range of 200 Hz. It is of the same order of magnitude as the expected beat note variation due to a magnetochiral index difference $\Delta n_{MC}=10^{-11}$. Moreover, like the magnetochiral index, $\Delta\nu_\varphi$ changes sign with respect to the direction of the magnetic field and depends on the handedness of the sample. Consequently, it may induce a systematic error during the measurement of the magnetochiral index. Thus, it has to be cancelled out to enable the detection of Δn_{MC} as small as 10^{-11} [24]. Experimentally, φ is minimized by using paired cells and by controlling the flatness of the baseline, when cells are filled with a racemic mixture. A typical baseline is reported in Fig. 5(c). Obtaining such a baseline allows the cancellation of the systematic effect efficiently, as shown in the next section.

V. INVESTIGATION OF THE MAGNETOCHIRAL EFFECT

We now focus on the experimental study of the magnetochiral index in limonene, including the investigation of polarization dependence and wavelength dispersion.

A. Amplitude and sign of the magnetochiral index

The measurement of the magnetochiral index of intracavity samples is carried out as follows. First, a racemic mixture is filled in both cells to test the flatness of the baseline [Fig. 5(c)]. Second, C_1 is filled with $R(+)$ limonene and C_2 is filled with $S(-)$ limonene. Then, we interchange the liquids to test the reversal of the sign of the beat note modulation. Figure 6 shows the typical evolution of the beat note frequency when the magnet rotates. The signals are averaged over 10 acquisitions. From the variation of the beat note frequency, and using Eq. (5), the variation of the magnetochiral optical index as a function of H is obtained. Figure 7 shows a typical recording of Δn_{MC} with respect to H. The observed linearity is in agreement with Eq. (5). It yields $\Delta n_{MC}=6.5(\pm2)\times10^{-10}$ T^{-1} for limonene with an e.e. of 82%. For limonene mixtures of e.e.=41%, we experimentally obtain $\Delta n_{MC}=3.2(\pm1)\times10^{-10}$ T^{-1}. Therefore, the linear dependence expected for the magnetochiral effect with respect to the enantiomeric excess is well observed. We point out that measurements were also performed with other compounds, namely

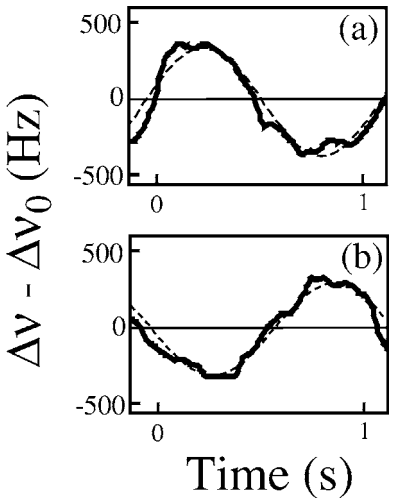

FIG. 6. Typical evolution of the beat note frequency. (a) $R(+)$ [respectively $S(-)$] limonene is filled in C_1 (respectively, C_2). (b) Samples interchanged in the cells with respect to (a). Dashed curves: sinusoidal fits. The baseline is shown in Fig. 5(c).

proline [7], which is one of the 20 proteic amino acids, and tartrates [24]. The experimental results, i.e., amplitude and sign of the magnetochiral birefringence, are in agreement with expression (3) and numerical calculations at the molecular level [15].

B. Polarization dependence of the magnetochiral effect

Symmetry considerations indicate that, in contrast to magnetic or natural optical activity, magnetochiral interaction is a scalar effect [1]. This point has been partially demonstrated because magnetochiral interaction has been shown to occur for unpolarized light in absorption and emission [5,11]. Conversely, for refraction, earlier experiments were performed with only one state of polarization [6,7]. Here, the polarizations of the probe beams are varied and Δn_{MC} is recorded. Moreover, this test could allow one to definitely discard the systematic error isolated (as discussed in the earlier section), which depends on polarization. To be able to monitor the inner state of polarization of the interferometer, two half-wave plates, L_1 and L_2, sandwich the cells. Their neutral axes are set at an angle γ relative to the x axis [Fig. 8(a)]. Between L_1 and L_2, the direction of the plane of polarization now makes an angle 2γ with respect to the x axis. However, this modification of the direction of polarization should not alter the beat note evolution. Figure 8(b) shows the beat note frequency versus time for three different orientations of the L_i's. As expected, the magnetochiral index does not depend on the incident polarization.

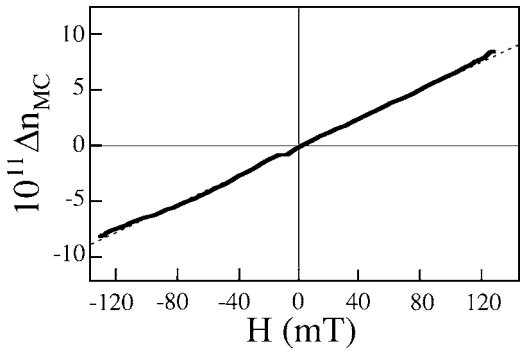

FIG. 7. Magnetochiral index of limonene Δn_{MC} as a function of the magnetic field H. Dashed line, linear fit.

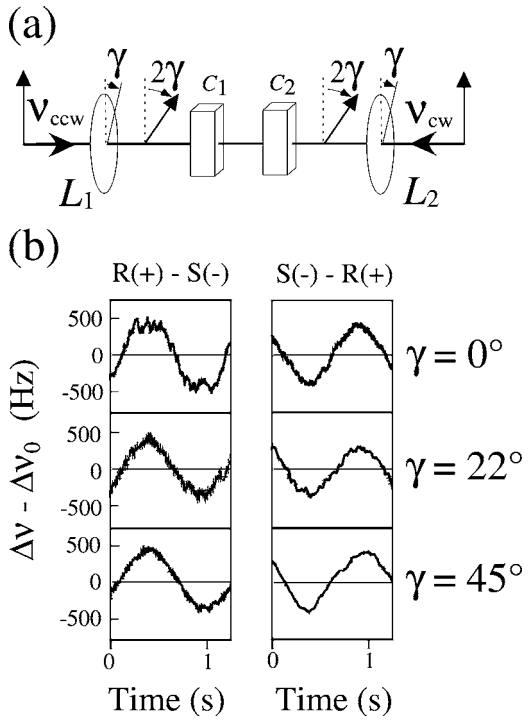

FIG. 8. (a) Experimental setup to vary the incident polarization on the cells. L_1, L_2, half-wave plates, with neutral axis at an angle γ with respect to the x axis. (b) Corresponding beat note evolution for three values of γ. The time evolutions in the left column correspond to $R(+)$ limonene in C_1 and $S(-)$ limonene in C_2. The liquids were interchanged to record the time evolutions in the right column.

C. Wavelength dispersion of the magnetochiral effect

To test the dependence of the magnetochiral anisotropy with respect to the wavelength, we modify the geometry of the interferometer to select different laser lines. Glass prisms are used as in linear single-line ion lasers [19]. The ring cavity of perimeter P=3.4 m now consists of two spherical mirrors M_1 and M_2 (radius of curvature R_c=6 m) and two glass prisms P_1 and P_2. Wavelength selection is made by changing the orientation of the prisms. For our setup, we obtain a single-line oscillation on the 488 nm ($4p^2D^0_{5/2} \rightarrow 4s^2P_{3/2}$) line or on the 514.5 nm ($4p^4D^0_{5/2} \rightarrow 4s^2P_{3/2}$) line. Assuming absorption bands in the far UV, and combining Eq. (2) and the expression $\theta(\lambda)=\Theta_0/(\lambda^2-\lambda_0^2)$ (Sec. II) for the angle of rotation due to optical activity, Δn_{MC} obeys the following wavelength dependence:

$$\Delta n_{MC} = -\frac{eH}{2\pi^2 mcL}\frac{\Theta_0\lambda_0^2\lambda^2}{(\lambda^2-\lambda_0^2)^2}. \tag{10}$$

For wavelengths far from absorption, the expected dispersion curve has a λ^{-2} shape, which is also obtained from full

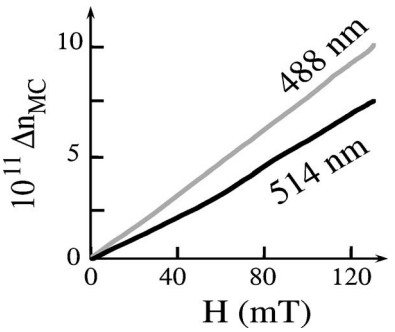

FIG. 9. Experimental evidence of magnetochiral dispersion: the magnetochiral index of $R(+)$ limonene, Δn_{MC}, is reported as a function of the magnetic field H. Gray line, $\lambda = 488$ nm; black line, $\lambda = 514$ nm.

quantum-mechanical considerations [9] or using a dipole-dipole interaction model [15]. Tuning the wavelength from 488 to 514.5 nm should lead to a decrease of 15% in the magnetochiral index. In Fig. 9, the results from the experiments performed on limonene are shown. When the wavelength is changed from 488 to 514.5 nm, the magnetochiral index decreases by a factor of 25% ($\pm 10\%$), in fair agreement with theoretical expectations (10).

VI. CONCLUSIONS

We have experimentally tested the different specific properties of the magnetochiral index. Indeed, the active interferometer we have built, which is based on an argon-ion ring laser, is well suited to identify and circumvent systematic errors that alter the signals, especially polarization-induced ones. Therefore, it yields true magnetochiral index measurements free from multiplicative or cascading effects. Furthermore, it has been shown that the use of the Sagnac and Fizeau effects, which are nonreciprocal and scalar as is the magnetochiral index, lead to beat note variations that can serve as independent calibrations. In addition, our apparatus is found to present high sensitivity to nonreciprocal index variations of the order of 10^{-12}.

Using this interferometer, we have shown that the magnetochiral index does not depend on the polarization of the input light. Moreover, producing gain with a multiline Ar^+ ion-discharge tube enables tuning the wavelength of the interferometer on different laser lines. This has allowed the determination of the wavelength dependence of the magnetochiral index. The magnetochiral index of $R(+)$ limonene has been measured to be $\Delta n_{MC} = -6.5(\pm 2) \times 10^{-10}\ \mathrm{T}^{-1}$. The magnetochiral indices of other molecules have also been probed with this apparatus, including a proteic amino acid, e.g., proline. The setup yields consistent results for the different tests carried out. Moreover, the experimental values are in agreement with theoretical calculations obtained from classical approaches [12,15].

We believe that the values obtained could be used to further test theoretical studies, including *ab initio* computations. Moreover, using calculations based on Kramers-Kronig relations for magnetochiral interaction, one could benefit from these values to deduce the associate values for absorption. Finally, these results may contribute to support the consequences on earth of the existence of the magnetochiral effect for unpolarized light, such as the origin of homochirality of life.

ACKNOWLEDGMENTS

The authors thank C. Pincet and C. Piel for their help during experimentation, and R.W. Boyd for fruitful discussions. This work was partially supported by the Conseil Régional de Bretagne in the framework of the Centre Laser et Applications à la Chimie et aux Télécommunications.

APPENDIX A: CALCULATION OF THE EIGENSTATES OF THE RING INTERFEROMETER

In this appendix, we derive the expression of the beat note frequency when the cells windows present linear birefringences. Using a vectorial description of the laser [22], the eigenfrequencies are calculated using the resonance conditions derived from Jones-matrix formalism for both waves [23]

$$\mathbf{M}^{ccw,cw} \cdot \mathbf{E} = \Lambda^{ccw,cw} \cdot \mathbf{E}, \tag{A1}$$

where $\mathbf{E}$ is the intracavity electric field, $\mathbf{M}^{cw}$ and $\mathbf{M}^{ccw}$ are the 2×2 Jones matrices for one round trip of the cavity, in the clockwise and counterclockwise directions, respectively, and Λ^{cw} and Λ^{ccw} are the corresponding eigenvalues. The four windows of the cells are labeled from 1–4 [see Fig. 1(b)]. Because of strain, each window labeled i may present a linear birefringence of retardance φ_i oriented at an angle ψ_i with respect to the x axis. The Jones matrix $\mathbf{L}(\varphi_i, \psi_i)$ associated to the window i is equal to $\mathbf{L}(\varphi_i, \psi_i) = \mathbf{R}(\psi_i) \cdot \mathbf{L}(\varphi_i, 0) \cdot \mathbf{R}(-\psi_i)$. In this equation, $\mathbf{R}(\psi_i)$ is the usual rotation matrix. $\mathbf{R}(\psi_i)$ and $\mathbf{L}(\varphi_i, 0)$ are given by [23]

$$\mathbf{R}(\psi_i) = \begin{pmatrix} \cos\psi_i & -\sin\psi_i \\ \sin\psi_i & \cos\psi_i \end{pmatrix} \text{ and } \mathbf{L}(\varphi_i, 0) = \begin{pmatrix} e^{i\varphi_i/2} & 0 \\ 0 & e^{-i\varphi_i/2} \end{pmatrix}. \tag{A2}$$

The two Brewster windows closing the tube behave as partial polarizers. The associated Jones matrix is

$$\mathbf{P}_x = \begin{pmatrix} \sqrt{1-\epsilon^2} & 0 \\ 0 & \epsilon \end{pmatrix}, \tag{A3}$$

with $\epsilon \ll 1$. We note θ_F (respectively, θ_{OA}) the rotation of the plane of polarization experienced by the ccw wave through the sample inside C_1 due to the Faraday effect (respectively, the optical activity). We consider that both Faraday rotation and optical activity are opposite in the two cells. Starting from the active medium, and neglecting the contributions of the active medium, i.e., using the cold-cavity approximation $\mathbf{M}^{cw}$ and $\mathbf{M}^{ccw}$ are equal to

$$\mathbf{M}^{ccw} = \mathbf{P}_x \cdot \mathbf{L}(\varphi_4, \psi_4)\mathbf{R}(-\theta_{OA})\mathbf{R}(-\theta_F)\mathbf{L}(\varphi_3, \psi_3) \times \mathbf{L}(\varphi_2, \psi_2)\mathbf{R}(\theta_{OA})\mathbf{R}(\theta_F)\mathbf{L}(\varphi_1, \psi_1)\mathbf{P}_x, \tag{A4a}$$

$$\mathbf{M}^{cw} = \mathbf{P}_x \cdot \mathbf{L}(\varphi_1, \psi_1)\mathbf{R}(-\theta_{OA})\mathbf{R}(\theta_F)\mathbf{L}(\varphi_2, \psi_2) \times \mathbf{L}(\varphi_3, \psi_3)\mathbf{R}(\theta_{OA})\mathbf{R}(-\theta_F)\mathbf{L}(\varphi_4, \psi_4)\mathbf{P}_x. \quad \text{(A4b)}$$

Poincaré theorem states that any combination of linear birefringences and rotators can be expressed as a combination of only one birefringence of retardance φ, rotated by an angle ψ and one rotator of angle χ [25]. Thus, we write

$$\mathbf{L}(\varphi_3, \psi_3) \cdot \mathbf{L}(\varphi_2, \psi_2) = \mathbf{L}(\varphi, \psi) \cdot \mathbf{R}(\chi), \quad \text{(A5a)}$$

$$\mathbf{L}(\varphi_2, \psi_2) \cdot \mathbf{L}(\varphi_3, \psi_3) = \mathbf{R}(-\chi) \cdot \mathbf{L}(\varphi, \psi). \quad \text{(A5b)}$$

Eigenvalues Λ^{ccw} and Λ^{cw} can be straightforwardly calculated using Eqs. (A2)–(A5). At first order in φ_i, ϵ, and Θ_F, the only nonzero eigenvalues correspond, as expected from the presence of Brewster windows, to linear eigenpolarization along the x axis. One finds

$$\Lambda^{ccw} = \cos(\chi) - i[\varphi_1 \cos(2\psi_1 - \chi) + \varphi_4 \cos(2\psi_4 + \chi) + \varphi \cos(2(\theta_{OA} + \theta_F - \psi) + \chi)], \quad \text{(A6a)}$$

$$\Lambda^{cw} = \cos(\chi) - i[\varphi_1 \cos(2\psi_1 - \chi) + \varphi_4 \cos(2\psi_4 + \chi) + \varphi \cos(2(\theta_{OA} - \theta_F - \psi) + \chi)]. \quad \text{(A6b)}$$

From this analysis, a new term $\Delta\nu_\varphi$ proportional to the difference of the arguments of the eigenvalues $\arg(\Lambda^{ccw}) - \arg(\Lambda^{cw})$, has to be added to the expression (5) of the beat note frequency. $\Delta\nu$ thus becomes

$$\Delta\nu = \Delta\nu_0 - \frac{cL}{\lambda P}\Delta n_{MC} + \Delta\nu_\varphi. \quad \text{(A7)}$$

$\Delta\nu_\varphi$ is equal to

$$\Delta\nu_\varphi = -\frac{c}{P}\frac{\varphi\theta_F}{\pi}\frac{\sin(2(\theta_{OA} - \psi) + \chi)}{\cos\chi}. \quad \text{(A8)}$$

Finally, if $\theta_{OA} \ll 1$, one obtains the expression (9) of the main text

$$\Delta\nu_\varphi \simeq \frac{c}{P}\frac{\varphi\theta_F}{\pi}\frac{\sin(2\psi - \chi)}{\cos\chi} - 2\frac{c}{P}\frac{\varphi\theta_F\theta_{OA}}{\pi}\frac{\cos(2\psi - \chi)}{\cos\chi}. \quad \text{(A9)}$$

[1] G. H. Wagnière, *Linear and Nonlinear Optical Properties of Molecules* (Verlag Helvetica Chimica Acta, Basel, Switzerland, 1993).

[2] S. Woźniak, Acta Phys. Pol. A **101**, 517 (2002).

[3] S. Coriani, M. Pecul, A. Rizzo, P. Jørgensen, and M. Jaszuski, J. Chem. Phys. **117**, 6417 (2002).

[4] F. A. Pinheiro and B. A. van Tiggelen J. Opt. Soc. Am. A **20**, 99 (2003).

[5] G. L. J. A. Rikken and E. Raupach, Nature (London) **390**, 493 (1997).

[6] P. Kleindienst and G. H. Wagnière, Chem. Phys. Lett. **288**, 89 (1998); N. G. Kalugin, P. Kleindienst, and G. H. Wagnière, Chem. Phys. **248**, 105 (1999).

[7] M. Vallet, R. Ghosh, A. Le Floch, T. Ruchon, F. Bretenaker, and J.-Y. Thépot, Phys. Rev. Lett. **87**, 183003 (2001).

[8] C. Koerdt, G. Düchs, and G. L. J. A. Rikken, Phys. Rev. Lett. **91**, 073902 (2003).

[9] L. D. Barron, *Molecular Light Scattering and Optical Activity*, 2nd ed (Cambridge University Press, Cambridge, U.K., 2004).

[10] G. H. Wagnière and A. Meier, Experientia **39**, 1090 (1983). For a review see B. L. Feringa and R. A. van Delden, Angew. Chem., Int. Ed. **38**, 3418 (1999).

[11] G. L. J. A. Rikken and E. Raupach, Nature (London) **405**, 932 (2000).

[12] N. B. Baranova, Y. V. Bogdanov, and B. Y. Zel'dovich, Opt. Commun. **22**, 243 (1977); N. B. Baranova and B. Y. Zel'dovich, Mol. Phys. **38**, 1085 (1979).

[13] M. P. Groenewege, Mol. Phys. **5**, 541 (1962); D. L. Portigal and E. Burstein, J. Phys. Chem. Solids **32**, 603 (1971); D. J. Caldwell and H. Eyring, *The Theory of Optical Activity* (Wiley Interscience/John Wiley & Sons, New York, 1971).

[14] G. H. Wagnière and A. Meier, Chem. Phys. Lett. **93**, 78 (1982); G. H. Wagnière, *ibid.* **110**, 546 (1984); L. D. Barron and J. Vrbancich, Mol. Phys. **51**, 715 (1984).

[15] T. Ruchon, D. Chauvat, M. Vallet, and A. Le Floch, in *Proceeding of the Eighth EPS Conference on Atomic and Molecular Physics* (Rennes, France, 2004).

[16] E. Charney, *The Molecular Basis of Optical Activity* (John Wiley & Sons, New York, 1979).

[17] G. L. J. A. Rikken and E. Raupach, Phys. Rev. E **58**, 5081 (1998).

[18] J. R. Wilkinson, Prog. Quantum Electron. **11**, 1 (1987).

[19] M. H. Dunn and J. N. Ross, Prog. Quantum Electron. **4**, 233 (1976).

[20] W. B. Bridges, A. N. Chester, A. S. Halsted, and J. V. Parker, Proc. IEEE **59**, 724 (1971).

[21] H. R. Bilger and A. T. Zavodny, Phys. Rev. A **5**, 591 (1972); G. A. Sanders and S. Ezekiel, J. Opt. Soc. Am. B **5**, 674 (1988).

[22] A. Le Floch and R. Le Naour, Phys. Rev. A **4**, 290 (1971).

[23] R. C. Jones, J. Opt. Soc. Am. **31**, 488 (1941).

[24] T. Ruchon, M. Vallet, J.-Y. Thépot, A. Le Floch, and R. W. Boyd, C. R. Phys. **5**, 273 (2004).

[25] H. J. Hurwitz and R. C. Jones, J. Opt. Soc. Am. **31**, 493 (1941).